A Device for Performing Lateral Conductance Measurements on Individual Double-Stranded DNA Molecules

Laurent D. Menard, Chad E. Mair, Michael E. Woodson, Jean Pierre Alarie, and J. Michael Ramsey*

Department of Chemistry, University of North Carolina at Chapel Hill, Chapel Hill, North Carolina 27599, United States

ABSTRACT

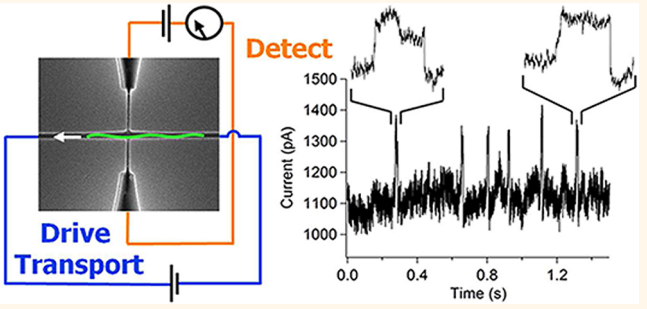

A nanofluidic device is described that is capable of electrically monitoring the driven translocation of DNA molecules through a nanochannel. This is achieved by intersecting a long transport channel with a shorter orthogonal nanochannel. The ionic conductance of this transverse nanochannel is monitored while DNA is electrokinetically driven through the transport channel. When DNA passes the intersection, the transverse conductance is altered, resulting in a transient current response. In 1 M KCl solutions, this was found to be a current enhancement of 5−25%, relative to the baseline transverse ionic current. Two different device geometries were investigated. In one device, the DNA was detected after it was fully inserted into and translocating through the transport nanochannel. In the other device, the DNA was detected while it was in the process of entering the nanochannel. It was found that these two conditions are characterized by different transport dynamics. Simultaneous optical and electrical monitoring of DNA translocation confirmed that the transient events originated from DNA transport through the nanochannel intersection.

KEYWORDS: DNA translocation · nanofluidics · nanochannels

Nanopores and nanochannels have recently been established as valuable fluidics tools for single-molecule studies, particularly of synthetic and biological macromolecules.[1−5] An important example is the use of biological protein pore complexes (*e.g.*, α-hemolysin) or pores fabricated in solid-state membranes to detect and characterize polynucleic acids.[6−10] Typically, single polynucleotides in electrolyte solution are electrokinetically driven through pores with constrictions that are marginally larger than the molecular cross sections of the analytes. This transport results in a deviation from the open pore ionic conductance, the amplitude and duration of which are characteristic of the analyte. Efforts are currently underway to develop methods realizing nucleotide sequence identification, allowing rapid, low cost, long read genomic sequencing of native DNA and RNA.[5,9,10]

Nanopores are typically characterized by an axial extent that is small relative to the macromolecule length. In contrast, nanochannels are usually defined as conduits having lengths commensurate with, or exceeding, the analyte's contour length. If the nanochannel's width and depth are smaller than the radius of gyration of the macromolecule, then confinement of the molecule in the nanochannel results in molecular extension, with the degree of extension increasing as nanochannel dimensions decrease. The molecule's extended configuration will consist of a string of blobs if the nanochannel width and depth are significantly greater than the persistence length of the polymer (∼50 nm for double-stranded DNA).[11] Another regime emerges when the nanochannel critical dimensions are smaller than the persistence length; the molecule, unable to fold back on itself, assumes a reflecting rod conformation.[12] In either case, the extension of a macromolecule along the length of a nanochannel facilitates single molecule characterizations. Specifically, the confinement of DNA in nanochannels has proven useful for sizing,[13,14] mapping,[15] separations,[16−18] and epigenetic analysis.[19] Such monitoring of DNA extension,[13,20,21] restriction sites,[15] or target binding sites[20,22] generally makes use of fluorescence microscopy.

The ability to monitor electrically DNA transport through nanochannels could offer a valuable and instrumentally simplistic complement to fluorescence microscopy. However, monitoring of the axial ionic current suffers from poor spatiotemporal resolution given the considerable length of the nanochannels.

* Address correspondence to jmramsey@unc.edu.

Received for review July 24, 2012 and accepted September 5, 2012.

Published online September 05, 2012
10.1021/nn303322r

Additionally, in cases where the channel is much longer than the analyte molecule, the relative response to analyte presence is small, yielding low signal-to-noise. In all systems (nanochannels and nanopores) in which the axial current is monitored, a single bias drives both DNA transport and the current flowing through the channel. As a result, translocation velocity and signal amplitude are highly correlated. Thus, the application of large biases to increase signal requires larger measurement bandwidths. Conversely, lower biases aimed at slowing translocation velocity mandate higher sensitivities and lower noise.

The development of devices containing opposed electrodes transverse to the transport nanopore or nanochannel has been proposed as a strategy for electrically monitoring DNA with high spatial resolution.[23−31] In such integrated devices, the nanochannel allows for the driven transport of DNA in a linear fashion through the electrode gap. As the DNA is driven past the electrodes, changes in the ionic or tunneling current across the electrodes are measured, providing a characterization of the DNA. The spatial and temporal resolution is dependent upon the degree of DNA extension, the width of the electrodes, and the characteristics of the various circuit elements. In the case of electrodes with single nanometer lateral extent and gap widths, it has been shown theoretically that the tunneling current can discriminate between the different bases in single-stranded DNA.[24] Such sensitivity of tunneling currents to nucleotide identity has also been demonstrated experimentally in scanning tunneling microscopy and molecular break junction studies.[29−33] An additional benefit of such a configuration is that two independent electric fields are employed, one to drive DNA transport and one to monitor passage through a detection region. The correlation between transport velocity and signal amplitude is consequently broken.

The challenges to integrating metal nanoelectrodes and nanofluidic components in a single device, however, are considerable. One implementation is to pattern nanoelectrodes or deposit nanowires onto a solid-state membrane and bisect the electrode by milling a nanopore through the membrane (Figure 1a).[26,27,34] Potential issues include the relatively fragile nature of these membrane-based devices and the large-area exposure of the biased electrodes to an electrolyte solution. Alternatively, electrodes can be interfaced to a nanochannel in a planar lab-on-a-chip type device, which is then sealed to form a closed network (Figure 1b).[28,35] In this system, realizing a highly planar surface, suitable for tightly sealing and isolating the individual device components is a primary challenge. In both of these electrode-based devices, electrochemically driven changes to the electrodes could render device performance unstable.[27] This is especially of concern for nanoelectrodes, where a large proportion of atoms are on the electrode surface. Such effects could be mitigated by appropriate materials selection or the addition of a redox mediator to the electrolyte solution.[36]

We have recently demonstrated the fabrication of nanofluidic devices having fluidic components with critical dimensions (width and depth) below 10 nm.[37] These channels are patterned using focused ion beam (FIB) milling, and the devices are sealed using fusion bonding. Using this capability, we fabricated devices having orthogonal, intersecting nanochannels as shown schematically in Figure 1c. One is a long nanochannel through which DNA molecules are electrokinetically driven while the transverse channel is a relatively short nanochannel through which the ionic conductance is monitored. Such devices are more readily sealed than those containing metal electrodes because the top surface remains highly planar. We speculated that such a device could realize the advantage described above of decoupling the transport-driving electric field from that used for detection. Additionally, spatial resolution would be sensitive to the electric field in the transverse nanochannel and defined by its lateral extent, similar to the case of metal electrodes. Since the electrode/electrolyte interfaces are macroscopic and removed from the detection site, electrochemical processes are of little concern. The ease of fabrication is expected to come at the cost of lower sensitivity compared to devices with metal nanoelectrodes. This results from the lower conductivity of electrolyte solutions compared to metals and the fact that the volume of the region in which the two channels intersect is a fraction of the total volume of the transverse channel. Despite these conditions, we observed relatively large perturbations in the transverse ionic conductance during driven DNA translocation. These transient current enhancements were analyzed to determine electrophoretic mobilities of DNA through the transport nanochannels that were consistent with previous results.[13,17,38] In varying the location of the transverse nanochannel (relative to the entrance of the transport channel), we found that the distributions of event duration differed for the cases in which DNA was fully confined within the nanochannel *versus* those in which DNA was in the process of entering the nanochannel. We believe these results will inform design paradigms for future sensing or sequencing devices containing either integrated metallic nanoelectrodes or nanofluidic channels. Finally, since the coplanarity of the device components and the quartz substrate are ideal for optical microscopy, we also monitored the translocation of fluorescently stained DNA molecules using microscopy and transverse ionic conductance simultaneously. These results showed good correlation between transverse ionic current perturbations and the transient presence of DNA in the nanochannel intersection.

RESULTS AND DISCUSSION

Results from three devices, having different dimensions, are presented in this Article. Figure 2 shows the general device architecture and representative

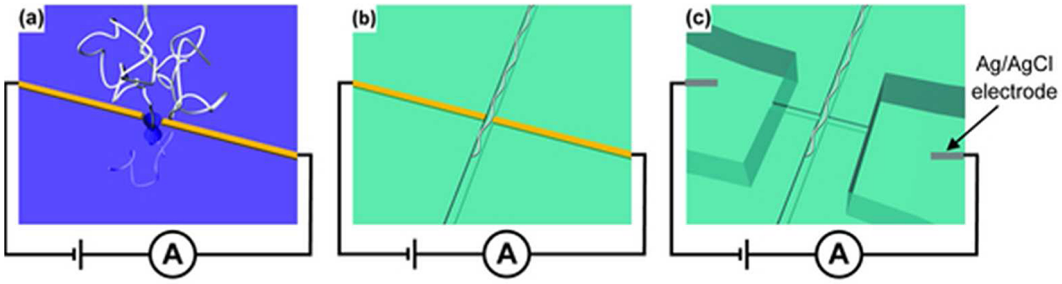

Figure 1. Schematic depictions of several devices for measuring transverse electrical signals during DNA translocation through a nanofluidic conduit. A device of the third class is the topic of this Article. (a) DNA is driven through a nanopore milled in the gap between two opposed nanoelectrodes. (b) DNA is extended in a nanochannel and is driven past a pair of metallic nanoelectrodes. (c) DNA is extended in a nanochannel and is driven past an intersecting nanofluidic channel through which the ionic current is measured.

micrographs of the nanochannel junction at different magnifications. The nanochannels are accessed by microchannels that are in turn accessed by ~100 μL reservoirs (Figure 2a). We note that the transverse nanochannels through which the ionic current is monitored are narrower than the transport channel (Figure 2c). This creates an entropic barrier to DNA translocating through the orthogonal channel, making continued translocation through the long transport channel more favorable. The characteristic dimensions of the devices used in these experiments are presented in Table 1.

We investigated the transport of double-stranded λ-phage DNA (48.5 kbp), which has a contour length of 16.8 μm, in KCl solutions. We discuss first the results of experiments conducted in 1 M KCl solutions in Devices A and B. A significant difference between the two devices is the distance between the entrance of the transport channel and the intersection of the transport and transverse nanochannels, 26.6 and 9.5 μm for Device A and Device B, respectively. The importance of these dimensions is discussed below.

Various control experiments were performed in which the baseline transverse ionic current was measured in the absence of DNA (both with and without a voltage applied across the transport channel) or once DNA had been introduced to the device but in the absence of an applied bias across the transport channel (Figure 3a,c). In these cases, a stable transverse ionic current free of transient events was observed. In contrast, when a DNA solution was introduced to the entrance of the transport nanochannel and a translocation-driving voltage applied, stochastically occurring current transients were observed in the transverse nanochannel (Figure 3b,d). These events are similar in shape and duration to those observed in the axial current of nanopores during the translocation of double-stranded λ-phage DNA. We believe they result from the translocation of single DNA molecules through the nanochannel intersection. Further evidence supporting this conclusion is detailed below.

The most conspicuous characteristic of the current transients observed in both devices is their directionality. We observed current enhancements in a high ionic strength 1 M KCl solution. In nanopore experiments in which the current is measured axial to translocation, current reductions or enhancements are observed in high and low ionic strength solutions, respectively.[39−41] In the former case, a reduced conductance is observed when DNA enters the pore due to the exclusion of the more mobile ions. In the latter case, the introduction of an elevated counterion concentration associated with the DNA actually enhances conductance. Curiously, we appear to observe an opposite effect, with current enhancements at high ionic strength and current reductions at low ionic strength (see below). We note that Liang and Chou reported transverse measurements of DNA in a device having integrated gold nanoelectrodes in which transient current reductions were observed in a low ionic strength buffer − 0.5 × TBE (45 mM Tris, 45 mM boric acid, 1 mM EDTA).[28] Also of note is a recent report by Liu *et al.* in which DNA translocation through single-walled carbon nanotubes resulted in current enhancements in 2 M KCl.[42] These results suggest that further studies are needed in order to better understand transient perturbations to ionic conduction in various nanoscale systems.

Individual events were characterized by their amplitude and duration. These data are presented for both devices in Figure 4. Similar to previous studies in both nanopores and nanochannels, we observed a number of events exhibiting multilevel current amplitudes, consistent with folded DNA molecules.[13,43] This population was quite small however (~5%) and the data analysis presented here is limited to single-level events. In Device A, the current amplitude of the transient events was 35 ± 5 pA,[44] or a 5% deviation from the baseline transverse current. The average event duration was 13 ± 3 ms (0.27 μs/bp) with apparent Gaussian distribution. From this event time, the electric field strength (820 V/cm), and the estimated extension length of the DNA molecules we can estimate the electrophoretic mobility of DNA in the 53 × 53 nm^2 transport nanochannels. We use the reflecting rod model of Odijk to estimate the molecule's extension length, *R*:

$$R = L\left(1 - 0.085\left[\left(\frac{A}{P}\right)^{(2/3)} + \left(\frac{B}{P}\right)^{(2/3)}\right]\right) \quad (1)$$

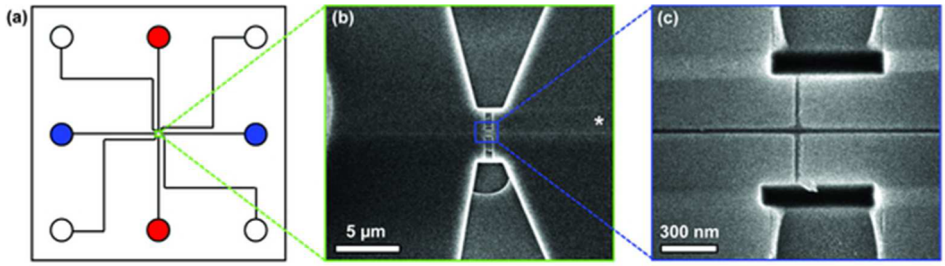

Figure 2. (a) Schematic of a crossed-nanochannel device (25 mm × 25 mm) showing the microchannels and reservoirs. The colored reservoirs indicate where voltages are applied. DNA transport is driven by applying a bias across the blue reservoirs and the voltage across the transverse (detection) nanochannel is applied at the red reservoirs. (b) Scanning electron micrograph of Device B. The asterisk (*) indicates the entrance to the transport nanochannel through which DNA is introduced. (c) High magnification scanning electron micrograph of the nanochannel intersection on Device B. The device was coated with a 2-nm thick AuPd film for SEM imaging, which was removed using aqua regia prior to device bonding.

TABLE 1. Nanochannel Dimensions in Lateral Conductance Devices

	transport nanochannel				transverse nanochannel		
device	width (nm)	depth (nm)	total length (μm)	distance,entrance to cross (μm)	width (nm)	depth (nm)	total length (μm)
A	53	53	50.4	26.6	25	43	2.2
B	31	28	21.7	9.5	22	59	0.5
C	200	180	80.0	41.8	35	160	2.1

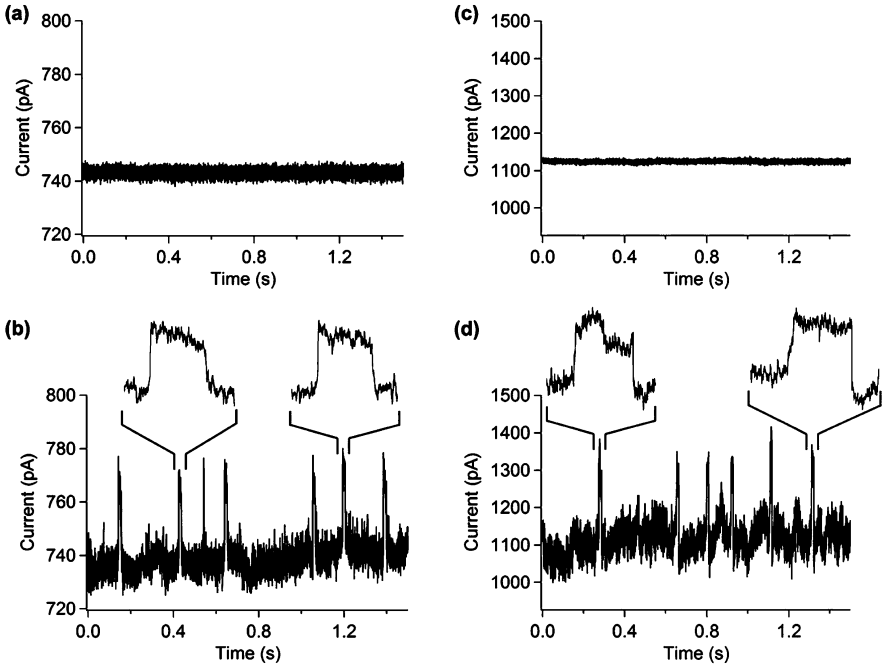

Figure 3. (a) Transverse ionic current measured in Device A when DNA was not being driven through the transport channel (50 mV applied). (b) Transverse ionic current in Device A detecting electrokinetically driven DNA transport. (c) Transverse ionic current measured in Device B when DNA was not being driven through the transport channel (100 mV applied). (d) Transverse ionic current measured in Device B when a voltage was applied across the transport channel, driving DNA translocations. The left-hand inset in panel d shows a relatively rare multilevel event consistent with DNA translocating in a folded state.

where L is the DNA contour length (16.8 μm), A and B are the nanochannel width and depth, respectively, and P is the persistence length (50 nm).[20] The Odijk model is appropriate for nanochannels having critical dimensions much smaller than the persistence length. In reality, for nanochannels with the dimensions described in this Article, molecular conformations are likely transitioning between the Odijk model and the blob model of de Gennes.[45] However, we also note that these are steady-state models and it has been observed that, as DNA molecules are driven into nanochannels, they are initially stretched beyond their equilibrium extension lengths.[46,47]

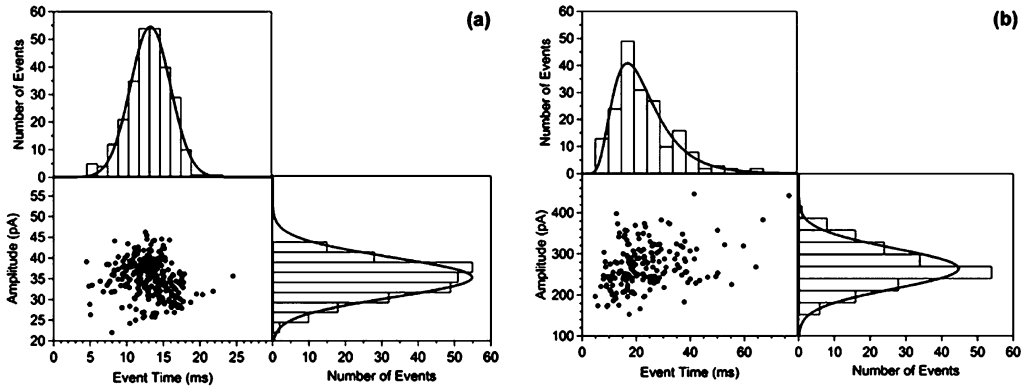

Figure 4. Event time and current amplitude histograms and scatter plots for (a) Device A and (b) Device B. All of the histograms were fit with normal distributions with the exception of that for event times measured in Device B, which was fit to a log-normal distribution. See text for details.

Given these considerations, extension lengths derived from the Odijk model offer a reasonable estimate for the length of DNA molecules passing the transverse nanochannel. In the case of the transport nanochannel of Device A this corresponds to an extension length of 13.8 μm. The estimated electrophoretic mobility is therefore 1.3 $\times$ 10^{-4} cm^2 V^{-1} s^{-1}, consistent with previously reported values.[13,17,38]

There are some significant differences apparent in the data collected from Device B. First, the current amplitude of the transient events is 271 $\pm$ 53 pA, or $\sim$27% of the baseline ionic current. The relatively low conductance of the ionic solution in the transverse nanochannel results in significant resistances in series with the region of the nanochannel sensitive to DNA-induced perturbations (*i.e.*, the intersection of the transport and transverse nanochannels). As a result, given the comparable cross sections of the transverse nanochannels in these two devices, this 5-fold greater sensitivity in Device B is commensurate with the 77% shorter transverse nanochannel in this device. The distribution of event times observed in Device B is distinct from that of Device A in that it is significantly skewed and broadened. Whereas the event time distribution of Device A is Gaussian and has a relative standard deviation of $\sim$23%, that of Device B is a log-normal distribution with a relative standard deviation of $\sim$53%. To understand this, we consider that the extension length estimated using the Odijk model in the 31 $\times$ 28 nm^2 transport nanochannel of Device B is 14.8 μm. This is longer than the distance from the transport nanochannel entrance to the intersection of the transport and transverse nanochannels (9.5 μm). In other words, λ-DNA molecules are not yet fully inserted into the nanochannel as the leading edges of the molecules are reaching the point of detection. Their velocity is therefore affected by dynamics that are a function of initial molecular configurations. We note that event time distributions are often skewed in nanopore experiments where molecular threading is a main component of the DNA translocation process.[48,49] This is in contrast to event distributions in devices where measurements are made on DNA molecules that are fully inserted into the nanochannels, as in Device A, which strongly limits the distribution of conformations. Consequently, following the design paradigm of Device A should yield more precise results for methods that characterize a population of DNA molecules based on the event time (*e.g.*, DNA sizing or probe mapping). For the sake of comparison with Device A we estimate an electrophoretic mobility of 0.6 $\times$ 10^{-4} cm^2 V^{-1} s^{-1} in Device B, using the estimated extension length, most probable event time (16 ms), and electric field strength (1470 V/cm). A lower mobility is expected given (1) the added drag experienced by the molecule because it is still entering the nanochannel and (2) the smaller size of the nanochannels and the consequently larger contribution of DNA/wall interactions.[50,51] We note that these mobility values are estimates, given the uncertainty in the λ-DNA extension lengths used for these calculations.

We turn now to a discussion of the simultaneous optical and electrical monitoring of DNA translocations in Device C. These experiments were performed in 125 mM KCl solutions because higher concentrations were found to disrupt the affinity for DNA of the intercalating fluorescent dye.[52,53] Our preliminary experiments suggested that the signal amplitude in the ionic conductance was considerably diminished under these conditions, consistent with reports of axial conductance perturbations observed in solid-state nanopores.[39] Consequently, we increased the nanochannel dimensions in Device C, thereby increasing the baseline transverse ionic conductance as well as the volume of DNA being probed. Figure 5 shows a representative series of fluorescence microscopy images and the ionic current that was concurrently monitored. The figure represents two consecutive events and not a concatenation of nonsequential data. Of 326 events recorded in either the optical or electrical modes, 168 (52%) were simultaneously detected in the

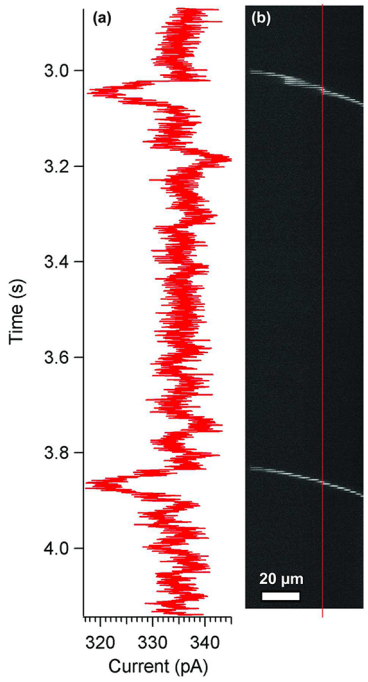

Figure 5. (a) Transverse ionic current measured in 125 mM KCl. (b) Series of frames recorded concurrently, showing the translocation of two YOYO-1 stained DNA molecules. Images were recorded at a frame rate of 234 frames/s. The vertical red line indicates the position of the transverse nanochannel.

ionic conductance measurement and fluorescence images, confirming a single DNA molecule translocated past the transverse nanochannel. A number of translocation events (92, 28%) were observed optically, with no detectable conductance response. These were typically small DNA fragments and we hypothesize that our device was not sufficiently sensitive to these fragments given the low ionic strength electrolyte solution. The remainder of events (66, 20%) were observed as ionic conductance perturbations with no corresponding optical event and may have been due to nonfluorescent species in the sample solution. In the 125 mM KCl solution, the current perturbations were reductions of 10 ± 5 pA from the baseline current of ~340 pA. This again represents a current response opposite to that observed in solid-state nanopores, as discussed above.[39] When experiments were performed on Device C in 1 M KCl (unstained λ-DNA, ionic conductance monitoring only) we again observed current enhancements in the transverse nanochannel, consistent with the results obtained using Devices A and B.

CONCLUSION

A new strategy is presented for monitoring DNA transport by probing the ionic conductance transverse to the direction of translocation. This is enabled by the nanofabrication of orthogonal, intersecting fluidic nanochannels using FIB milling. This strategy avoids some of the fabrication challenges posed in interfacing metal electrodes to nanofluidic channels for the purposes of making similar transverse measurements. The transport of single λ-DNA molecules was observed as transient current enhancements in high ionic strength electrolyte solutions. The durations of these stochastic transient signals were analyzed to estimate the electrophoretic mobility of DNA in the transport nanochannels. It was observed that the shapes of the event time distributions are dependent upon the location of the transverse sensing region relative to the transport nanochannel entrance. Translocations were also detected as current reductions in lower ionic strength solutions compatible with fluorescent staining of DNA molecules using intercalating dyes. DNA transport was monitored using fluorescence microscopy and the transverse ionic conductance simultaneously, showing good correlation between the ionic conductance perturbations and the transport of DNA through the nanochannel intersection. With their ease of fabrication and electrically based mode of detection, these nanofluidic devices have potential as low cost, simple, yet powerful platforms for applications such as DNA sizing and mapping.

METHODS

Device Fabrication. The details of device fabrication have been reported elsewhere.[37] Briefly, the microfluidic elements of a device are patterned in a quartz substrate using photolithography and isotropic wet etching techniques. Then the nanochannels are milled into the quartz substrate through a 120-nm thick chromium film using FIB milling (Helios NanoLab DualBeam, FEI Company). After removing the chromium film with an etching solution (Chromium Mask Etchant, Transene Company, Inc.), a quartz coverslip is fusion bonded to the substrate to seal the fluidic network.

Ionic Conductance Detection in 1 M KCl. In experiments using unstained DNA, the micro- and nanochannels were hydrodynamically filled with an electrolyte solution (1 M KCl, 10 mM Tris, 1 mM EDTA). Solutions of λ-DNA (5 ng/μL) were prepared in this same electrolyte and then introduced *via* the microchannel accessing the entrance of the long transport nanochannel. The ionic current through the short transverse nanochannel was driven and monitored using an Axopatch 200B patch clamp amplifier (Molecular Devices). A voltage of 50−200 mV was applied to macroscopic Ag/AgCl electrodes immersed in the appropriate reservoirs (red reservoirs in Figure 2a). Single molecules of λ-DNA were electrokinetically driven through the transport nanochannel by biasing platinum electrodes immersed in the reservoirs (blue reservoirs in Figure 2a). A floating power source was used to drive transport in these experiments with voltages of 4−10 V. The experiments were performed at room temperature (24.3 ± 0.5 °C) without active temperature control. These experiments were performed using Devices A and B.

Simultaneous Optical and Electrical Detection in 125 mM KCl. Experiments in which DNA translocation was monitored both optically and electrically were similarly carried out, but with several modifications. The λ-DNA was fluorescently stained with the intercalating dye YOYO-1 (Invitrogen) at a base pair-to-dye ratio of 5:1. The electrolyte solution used was 125 mM KCl, 10 mM Tris, 1 mM EDTA with an added 4% by volume of β-mercaptoethanol as a radical scavenger that reduces photoinduced

damage. The experiment was performed on an Eclipse TE2000-U inverted microscope (Nikon) using a 100 × /1.4 NA oil immersion objective (Nikon). Fluorescence was excited at 472 nm using a mercury arc lamp filtered through a band-pass filter, with emission collected at 520 nm (Semrock). Images were acquired using a Cascade II EM-CCD camera (Photometrics) recording at frame rates of at least 200 frames s^{-1}. Recording of the transverse ionic conductance and of the fluorescence images were triggered simultaneously. The experiments were performed at room temperature without active temperature control. These experiments were performed using Device C.

Conflict of Interest: The authors declare no competing financial interest.

Acknowledgment. This work was sponsored in part by a grant from the National Human Genome Research Institute, National Institutes of Health (R01HG02647-05). We are grateful to Prof. Michael Rubinstein for helpful discussions. We also thank the staff of the Chapel Hill Analytical and Nanofabrication Laboratory (CHANL) for their support.

REFERENCES AND NOTES

1. Abgrall, P.; Nguyen, N. T. Nanofluidic Devices and Their Applications. *Anal. Chem.* **2008**, *80*, 2326–2341.
2. Douville, N.; Huh, D.; Takayama, S. DNA Linearization through Confinement in Nanofluidic Channels. *Anal. Bioanal. Chem.* **2008**, *391*, 2395–2409.
3. Kasianowicz, J. J.; Robertson, J. W. F.; Chan, E. R.; Reiner, J. E.; Stanford, V. M. Nanoscopic Porous Sensors. *Annu. Rev. Anal. Chem.* **2008**, *1*, 737–766.
4. Schoch, R. B.; Han, J.; Renaud, P. Transport Phenomena in Nanofluidics. *Rev. Mod. Phys.* **2008**, *80*, 839–883.
5. Branton, D.; Deamer, D. W.; Marziali, A.; Bayley, H.; Benner, S. A.; Butler, T.; Di Ventra, M.; Garaj, S.; Hibbs, A.; Huang, X.; *et al.* The Potential and Challenges of Nanopore Sequencing. *Nat. Biotechnol.* **2008**, *26*, 1146–1153.
6. Kasianowicz, J. J.; Brandin, E.; Branton, D.; Deamer, D. W. Characterization of Individual Polynucleotide Molecules Using a Membrane Channel. *Proc. Natl. Acad. Sci. U.S.A.* **1996**, *93*, 13770–13773.
7. Mathé, J.; Aksimentiev, A.; Nelson, D. R.; Schulten, K.; Meller, A. Orientation Discrimination of Single-Stranded DNA inside the α-Hemolysin Membrane Channel. *Proc. Natl. Acad. Sci. U.S.A.* **2005**, *102*, 12377–12382.
8. Derrington, I. M.; Butler, T. Z.; Collins, M. D.; Manrao, E.; Pavlenok, M.; Niederweis, M.; Gundlach, J. H. Nanopore DNA Sequencing with MspA. *Proc. Natl. Acad. Sci. U.S.A.* **2010**, *107*, 16060–16065.
9. Cherf, G. M.; Lieberman, K. R.; Rashid, H.; Lam, C. E.; Karplus, K.; Akeson, M. Automated Forward and Reverse Ratcheting of DNA in a Nanopore at 5-Å Precision. *Nat. Biotechnol.* **2012**, *30*, 344–348.
10. Manrao, E. A.; Derrington, I. M.; Laszlo, A. H.; Langford, K. W.; Hopper, M. K.; Gillgren, N.; Pavlenok, M.; Niederweis, M.; Gundlach, J. H. Reading DNA at Single-Nucleotide Resolution with a Mutant MspA Nanopore and phi29 DNA Polymerase. *Nat. Biotechnol.* **2012**, *30*, 349–353.
11. Daoud, M.; de Gennes, P. G. Statistics of Macromolecular Solutions Trapped in Small Pores. *J. Phys. (Paris)* **1977**, *38*, 85–93.
12. Odijk, T. On the Statistics and Dynamics of Confined or Entangled Stiff Polymers. *Macromolecules* **1983**, *16*, 1340–1344.
13. Reccius, C. H.; Stavis, S. M.; Mannion, J. T.; Walker, L. P.; Craighead, H. G. Conformation, Length, and Speed Measurements of Electrodynamically Stretched DNA in Nanochannels. *Biophys. J.* **2008**, *95*, 273–286.
14. Foquet, M.; Korlach, J.; Zipfel, W.; Webb, W. W.; Craighead, H. G. DNA Fragment Sizing by Single Molecule Detection in Submicrometer-Sized Closed Fluidic Channels. *Anal. Chem.* **2002**, *74*, 1415–1422.
15. Riehn, R.; Lu, M.; Wang, Y.-M.; Lim, S. F.; Cox, E. C.; Austin, R. H. Restriction Mapping in Nanofluidic Devices. *Proc. Natl. Acad. Sci. U.S.A.* **2005**, *102*, 10012–10016.
16. Han, J.; Craighead, H. G. Separation of Long DNA Molecules in a Microfabricated Entropic Trap Array. *Science* **2000**, *288*, 1026–1029.
17. Cross, J. D.; Strychalski, E. A.; Craighead, H. G. Size-Dependent DNA Mobility in Nanochannels. *J. Appl. Phys.* **2007**, *102*, 024701.
18. Strychalski, E. A.; Lau, H. W.; Archer, L. A. Nonequilibrium Separation of Short DNA Using Nanoslit Arrays. *J. Appl. Phys.* **2009**, *106*, 024915.
19. Cipriany, B. R.; Zhao, R.; Murphy, P. J.; Levy, S. L.; Tan, C. P.; Craighead, H. G.; Soloway, P. D. Single Molecule Epigenetic Analysis in a Nanofluidic Channel. *Anal. Chem.* **2010**, *82*, 2480–2487.
20. Jo, K.; Dhingra, D. M.; Odijk, T.; de Pablo, J. J.; Graham, M. D.; Runnheim, R.; Forrest, D.; Schwartz, D. C. A Single-Molecule Barcoding System Using Nanoslits for DNA Analysis. *Proc. Natl. Acad. Sci. U.S.A.* **2007**, *104*, 2673–2678.
21. Reisner, W.; Morton, K. J.; Riehn, R.; Wang, Y. M.; Yu, Z.; Rosen, M.; Sturm, J. C.; Chou, S. Y.; Frey, E.; Austin, R. H. Statics and Dynamics of Single DNA Molecules Confined in Nanochannels. *Phys. Rev. Lett.* **2005**, *94*, 196101.
22. Wang, Y. M.; Tegenfeldt, J. O.; Reisner, W.; Riehn, R.; Guan, X.-J.; Guo, L.; Golding, I.; Cox, E. C.; Sturm, J.; Austin, R. H. Single-Molecule Studies of Repressor−DNA Interactions Show Long-Range Interactions. *Proc. Natl. Acad. Sci. U.S.A.* **2005**, *102*, 9796–9801.
23. Zwolak, M.; Di Ventra, M. Electronic Signature of DNA Nucleotides *via* Transverse Transport. *Nano Lett.* **2005**, *5*, 421–424.
24. Lagerqvist, J.; Zwolak, M.; Di Ventra, M. Fast DNA Sequencing *via* Transverse Electronic Transport. *Nano Lett.* **2006**, *6*, 779–782.
25. Lagerqvist, J.; Zwolak, M.; Di Ventra, M. Influence of the Environment and Probes on Rapid DNA Sequencing *via* Transverse Electronic Transport. *Biophys. J.* **2007**, *93*, 2384–2390.
26. Fischbein, M. D.; Drndić, M. Sub-10 nm Device Fabrication in a Transmission Electron Microscope. *Nano Lett.* **2007**, *7*, 1329–1337.
27. Gierhart, B. C.; Howitt, D. G.; Chen, S. J.; Zhu, Z.; Kotecki, D. E.; Smith, R. L.; Collins, S. D. Nanopore with Transverse Nanoelectrodes for Electrical Characterization and Sequencing of DNA. *Sens. Actuators B* **2008**, *132*, 593–600.
28. Liang, X.; Chou, S. Y. Nanogap Detector Inside Nanofluidic Channel for Fast Real-Time Label-Free DNA Analysis. *Nano Lett* **2008**, *8*, 1472–1476.
29. Tsutsui, M.; Matsubara, K.; Ohshiro, T.; Furuhashi, M.; Taniguchi, M.; Kawai, T. Electrical Detection of Single Methylcytosines in a DNA Oligomer. *J. Am. Chem. Soc.* **2011**, *133*, 9124–9128.
30. Tsutsui, M.; Rahong, S.; Iizumi, Y.; Okazaki, T.; Taniguchi, M.; Kawai, T. Single-Molecule Sensing Electrode Embedded In-Plane Nanopore. *Sci. Rep.* **2011**, *1*, 46.
31. Tsutsui, M.; Taniguchi, M.; Yokota, K.; Kawai, T. Identifying Single Nucleotides by Tunnelling Current. *Nat. Nanotechnol.* **2010**, *5*, 286–290.
32. Chang, S.; Huang, S.; He, J.; Liang, F.; Zhang, P.; Li, S.; Chen, X.; Sankey, O.; Lindsay, S. Electronic Signatures of All Four DNA Nucleosides in a Tunneling Gap. *Nano Lett.* **2010**, *10*, 1070–1075.
33. Tanaka, H.; Kawai, T. Partial Sequencing of a Single DNA Molecule with a Scanning Tunnelling Microscope. *Nat. Nanotechnol.* **2009**, *4*, 518–522.
34. Taniguchi, M.; Tsutsui, M.; Yokota, K.; Kawai, T. Fabrication of the Gating Nanopore Device. *Appl. Phys. Lett.* **2009**, *95*, 123701.
35. Tsutsui, M.; Taniguchi, M.; Kawai, T. Transverse Field Effects on DNA-Sized Particle Dynamics. *Nano Lett.* **2009**, *9*, 1659–1662.
36. Lemay, S. G. Nanopore-Based Biosensors: The Interface between Ionics and Electronics. *ACS Nano* **2009**, *3*, 775–779.
37. Menard, L. D.; Ramsey, J. M. The Fabrication of Sub-5-nm Nanochannels in Insulating Substrates Using Focused Ion Beam Milling. *Nano Lett.* **2011**, *11*, 512–517.
38. Campbell, L. C.; Wilkinson, M. J.; Manz, A.; Camilleri, P.; Humphreys, C. J. Electrophoretic Manipulation of Single

DNA Molecules in Nanofabricated Capillaries. *Lab Chip* **2004**, *4*, 225–229.
39. Smeets, R. M. M.; Keyser, U. F.; Krapf, D.; Wu, M.-Y.; Dekker, N. H.; Dekker, C. Salt Dependence of Ion Transport and DNA Translocation through Solid-State Nanopores. *Nano Lett.* **2006**, *6*, 89–95.
40. Chang, H.; Kosari, F.; Andreadakis, G.; Alam, M. A.; Vasmatzis, G.; Bashir, R. DNA-Mediated Fluctuations in Ionic Current through Silicon Oxide Nanopore Channels. *Nano Lett.* **2004**, *4*, 1551–1556.
41. Cui, S. Current Blockade in Nanopores in the Presence of Double-Stranded DNA and the Microscopic Mechanisms. *J. Phys. Chem. B* **2010**, *114*, 2015–2022.
42. Liu, H.; He, J.; Tang, J.; Liu, H.; Pang, P.; Cao, D.; Krstic, P.; Joseph, S.; Lindsay, S.; Nuckolls, C. Translocation of Single-Stranded DNA through Single-Walled Carbon Nanotubes. *Science* **2010**, *327*, 64–67.
43. Storm, A. J.; Chen, J. H.; Zandbergen, H. W.; Dekker, C. Translocation of Double-Strand DNA through a Silicon Oxide Nanopore. *Phys. Rev. E* **2005**, *71*, 051903.
44. This value and all subsequent values reported in this format are reported as mean ± standard deviation.
45. Odijk, T. Scaling Theory of DNA Confined in Nanochannels and Nanoslits. *Phys. Rev. E* **2008**, *77*, 060901.
46. Mannion, J. T.; Reccius, C. H.; Cross, J. D.; Craighead, H. G. Conformational Analysis of Single DNA Molecules Undergoing Entropically Induced Motion in Nanochannels. *Biophys. J.* **2006**, *90*, 4538–4545.
47. Balducci, A.; Hsieh, C.-C.; Doyle, P. S. Relaxation of Stretched DNA in Slitlike Confinement. *Phys. Rev. Lett.* **2007**, *99*, 238102.
48. Meller, A.; Branton, D. Single Molecule Measurements of DNA Transport through a Nanopore. *Electrophoresis* **2002**, *23*, 2583–2591.
49. Bates, M.; Burns, M.; Meller, A. Dynamics of DNA Molecules in a Membrane Channel Probed by Active Control Techniques. *Biophys. J.* **2003**, *84*, 2366–2372.
50. Balducci, A.; Mao, P.; Han, J.; Doyle, P. S. Double-Stranded DNA Diffusion in Slitlike Nanochannels. *Macromolecules* **2006**, *39*, 6273–6281.
51. Strychalski, E. A.; Levy, S. L.; Craighead, H. G. Diffusion of DNA in Nanoslits. *Macromolecules* **2008**, *41*, 7716–7721.
52. Günther, K.; Mertig, M.; Seidel, R. Mechanical and Structural Properties of YOYO-1 Complexed DNA. *Nucleic Acids Res.* **2010**, *38*, 6526–6532.
53. Larsson, A.; Carlsson, C.; Jonsson, M. Characterization of the Binding of YO to $[poly(dA\text{-}dT)]_2$ and $[poly(dG\text{-}dC)]_2$, and of the Fluorescent Properties of YO and YOYO Complexed with the Polynucleotides and Double-Stranded DNA. *Biopolymers* **1995**, *36*, 153–167.